NUMERICAL SIMULATION OF MATERIAL FLOW IN AA6082 DURING FRICTION STIR SPOT WELDING

Z. Gao[1*] – P. Wang[1] – D. Cheng[1] – J. Niu[1, 2] – C. Sommitsch[3]

[1]School of Materials Science and Engineering, Henan Polytechnic University, Henan, Jiaozuo, 454003, P. R. China
[2]Henan Jingtai Aerospace High-Novel Materials Technology Co., Ltd, Henan, Jiaozuo, 454003, P. R. China
[3]Institute for Materials Science and Welding, Graz University of Technology – Graz, 8010, Austria

ARTICLE INFO

***Article history*:**
Received: 15.12.2014.
Received in revised form: 04.02.2015.
Accepted: 06.02.2015.

Keywords:
Friction stir spot welding
AA 6082
Material flow
Numerical simulation
Effective strain rate

Abstract:

Friction stir spot welding (FSSW) is a new solid state joining technology based on the linear friction stir welding which can be used to replace the conventional resistance spot welding as well as riveting. However, some key problems such as heat transfer and thermoplastic material flow have not yet been studied sufficiently and block the application of this advanced technology. This paper presents the coupled thermo-mechanical viscoplastic finite element formulation based on the character of FSSW. The model was calibrated by comparing temperature history between simulation results and experimental data and subsequently used to investigate the effective strain rate and material flow in joint. The temperature study showed that the simulation and experiment results coincided well with each other thus proofing the correctness of the model. The simulation results showed that the effective strain rate distribution were not uniform. The material close to the pin's cylindrical surface had a higher effective strain rate than that of the other material. The materials in weld centre mainly experienced a compression process and the other material under the tool experienced both compression and shear process.

1 Introduction

Friction stir welding (FSW) is a solid state joining process to obtain high quality joints. During FSW, heating is provided mainly by / due to the friction energy. Meanwhile, the energy from plastic deformation is also a part of heating energy [1-3]. Friction stir spot welding (FSSW) is a new solid state joining technology, which is based on the linear friction stir welding and it can be used to replace the conventional resistance spot welding as well as riveting. FSSW has great advantages in the area of light alloy joint, especially for aluminum. It has won the favor of customers and recognition from the areas of aerospace, automobile, shipbuilding industries and so on [4]. The FSSW process may be divided into four main phases, namely, touch down, plunge, dwell and retraction,

[*] Corresponding author. Tel.: 0086-13839134383; fax: 0086-391-3986901
E-mail address: mrgaozeng@163.com

which can be found in Fig. 1. As the process begins, the rotating tool commences to touch down with vertical down force. In the meantime, frictional heat is generated at the interface between tool pin and work piece. With the plunge/by plunging, the rotating tool is held in that position for a pre-determined finite time (dwell phase) when reaching the desired plunge depth. Subsequent to that, the rotating tool is then retracted from the welded joint leaving behind a friction stir spot weld. Generally, FSSW can be considered as a transient process due to its short cycle time [5-7]. During FSSW, tool penetration and the dwell period essentially determine the heat generation, materials plasticization around the pin, weld geometry and therefore the mechanical properties of the joint.

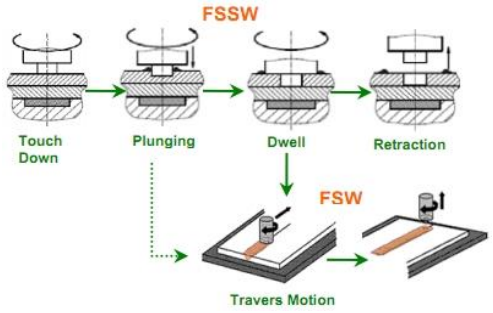

Figure 1. Process phases during FSSW and FSW.

When the temperature in work piece is high enough, the material will become soft and then it can create sticking condition at that interface between the tool and work piece. In that condition, the work piece material behaves like a viscous fluid at the interface. With the domination of sticking condition, the heat input due to friction decreases. The overall energy input is decreased and hence the temperature decreases [8, 9].

2 Numerical simulation of FSSW

The model developed in this study is three dimensional. The commercial FEA software DEFORM-3D^{TM}, Lagrangian implicit code designed for metal forming processes, has been utilized to model the FSSW process. Considering the application condition of FSSW, hot rolling aluminum alloy AA6082 without heat treatment was used in both simulation and experimental validation. The main objective of current numerical simulation is to understand the temperature distribution, effective strain rate and material flow in the joint of AA6082. So the simplest possible model is developed, i.e., simple tool geometries without threads and other features. The model consists of three parts: tool, work piece and back plate, as shown in Fig. 2. The shoulder and pin diameter of the tool is 11 mm and 5 mm, respectively. The height of the tool is 2 mm. Besides, the thickness of the work piece is 4 mm. The work piece was modeled as a rigid-viscoplastic material and the tool as well as the back plate was assumed as rigid bodies. One single sheet was used as the work piece instead of 2 sheets, in order to avoid contact instability due to the intermittent contact at the interface between sheets [10]. During simulation, the typical experimental process parameters were used as following: rotational speed 2400 r/min, plunge depth 2.2 mm, plunge rate 72 mm/min and dwell time 1 s.

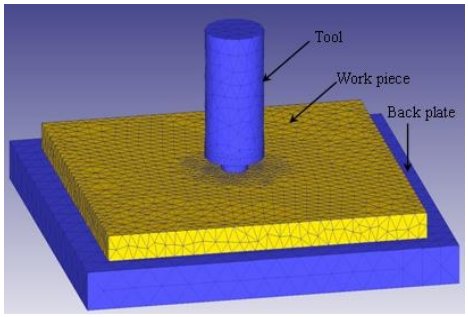

Figure 2. Schematic illustration of the assembly.

Fig. 3 shows the material flow stress data of AA6082 at 500 °C. The true stress-strain data for the material flow were obtained from isothermal compression tests at temperatures from 300 to 550 °C and strain rates from 0.001 to 100 s^{-1}.

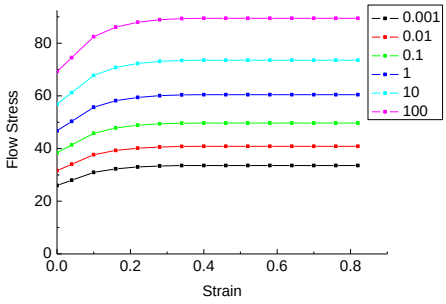

Figure 3. Flow stress-strain curves for AA 6082 used in the model.

As far as the thermal characteristics of AA6082 concerns, the following constant values were utilized: heat capacity 889 [J/kg K], convection coefficient 20 [W/m^2 K], emissivity 700 [W/m^2 K^4]. Thermal conductivity was taken into account as a function of temperature as shown in Table 1.

Table 1. Thermal conductivity of AA6082

Temperature (°C)	20	100	200
Thermal conductivity (W/m K)	215	212	215
Temperature (°C)	300	400	500
Thermal conductivity (W/m K)	216	208	202

The shear friction model was selected in this study. The friction force is defined by:

$$f = m\,k, \qquad (1)$$

where f denotes the frictional stress, k the shear yield strength and m the friction factor [11]. This states that the friction is a function of the yield stress of the deforming body. To select an appropriate friction factor, it is very important because it has a significant influence on the heat generation. If the friction factor is too small, heat generation will be too low to plastify the materials and to weld them, while in the simulation, too large friction factors may result in an unreasonable thermal field. For the friction factor calibration, the temperature history derived from simulations was compared with experimental data.

3 Results and discussion

3.1 Temperature distribution in FSSW joint

In order to validate the accuracy of the numerical model, the temperature history was compared at two points. The measured points located at the surface of work piece. As it can be seen from Fig. 4, a good match could be achieved between the predicted and measured temperature history. It indicates that the numerical model is appropriate. The temperature increases slowly at the beginning of the plunge. The main reason for that is the small friction area and large distance to the measuring point. The temperature increases rapidly after making contacts between shoulder and work piece. Fig. 5 shows the temperature distribution in work piece at the end of process. It can be seen that the peak temperature value is 526 °C. It is about 0.86 times the homologous melting temperature (in Kelvin) of the base metal. The temperature distribution is symmetric around the tool and the higher temperature appears at the interface between tool and work piece.

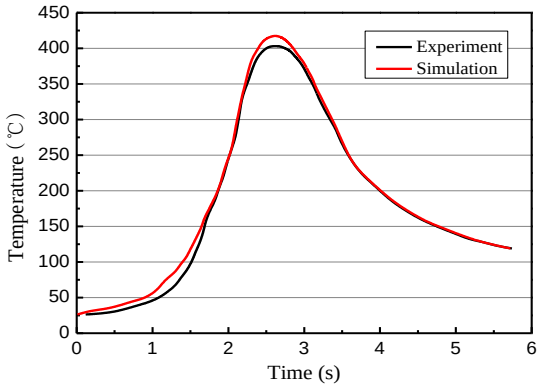

(a)

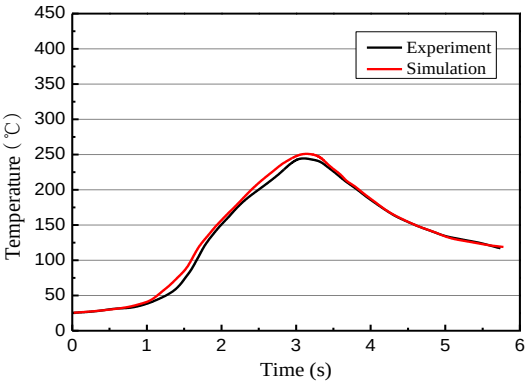

(b)

Figure 4. Temperature comparison between the numerical simulation and experiment: (a) Point 1, 1 mm away from the outer edge of the shoulder, (b) Point 2, 3 mm away from the outer edge of the shoulder.

3.2 Effective strain rate distribution during the different phase of FSSW process

Fig. 6 shows the effective strain rate distribution during the FSSW process. It can be seen from Fig. 6 (a), at the very beginning of plunging, the effective strain rate is quite low because there is not enough heat to plastify the material.

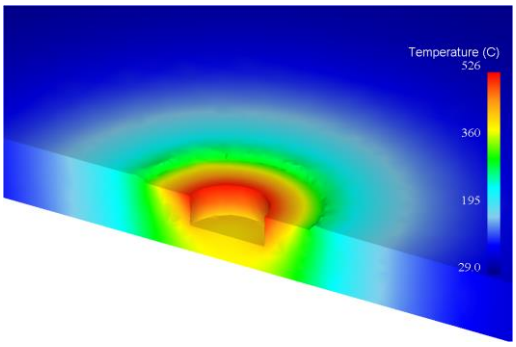

Figure 5. Temperature distribution in work piece at the end of process.

By plunging the tool, the work piece receives more and more heat during friction, which results in softening of the material, and then the material can rotate with the tool's rotation. Therefore, the material obtains a high effective strain rate. Before the shoulder contacts with the work piece, the material has already been plasticized and it can obtain a very high effective strain rate, shown in Fig. 6 (b). Fig. 6 (c) shows the even higher effective strain rate after the shoulder contact with the work piece. Like the character of FSSW, the material under the tool rotates with the tool's rotation, which results in local high effective strain rates. The regions with high effective strain rates are mainly located at the periphery of the pin rather than the place under the shoulder. Similarly, Fig. 6 (d) shows the effective strain rate at the dwell stage. During this stage, the material still deforms with the rotation of the tool due to the viscoplastic condition.

3.3 Material flow analysis in FSSW joint

During FSSW, tool plunging and dwell period essentially determine the heat generation, material plasticization around the pin, weld geometry and therefore the mechanical properties of the welded joint. By using the point tracking method, the material flow can be investigated in work piece during FSSW process.

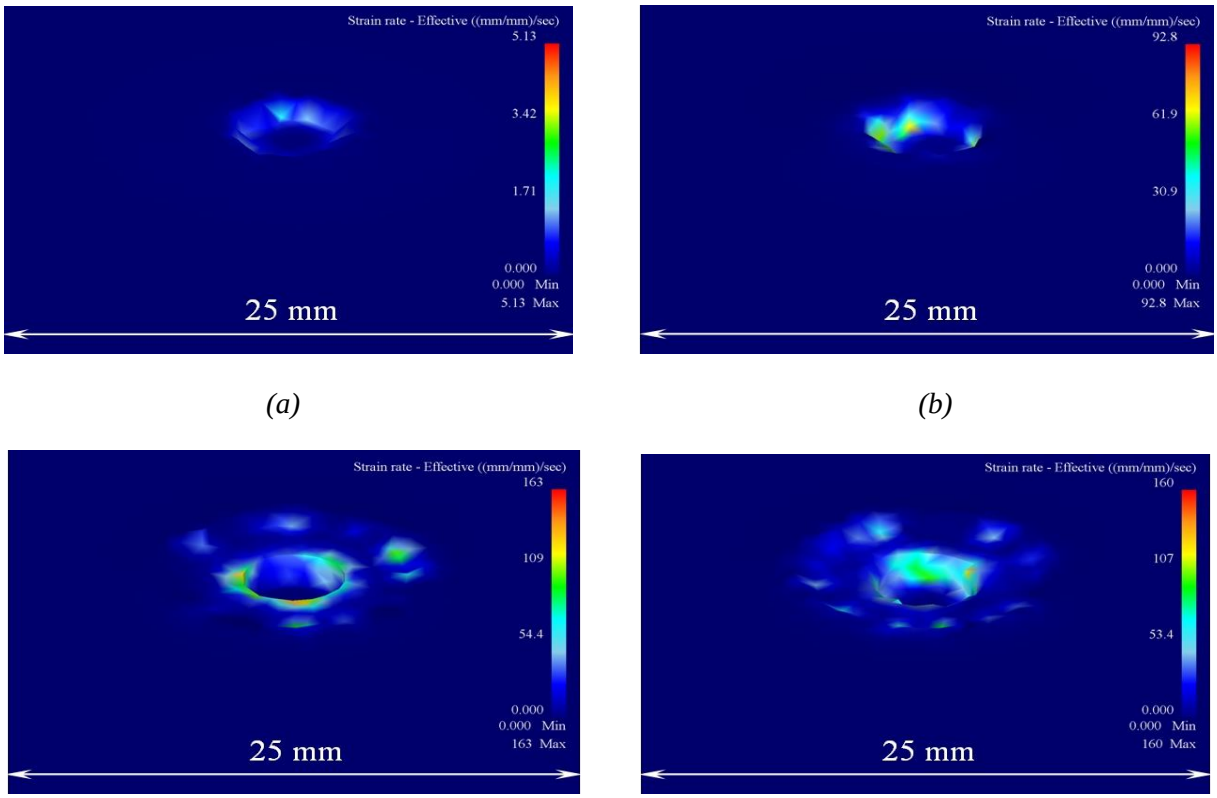

Figure 6. Effective strain rate distribution at the moment of (a) beginning; (b) plunging; (c) making contacts between shoulder and work piece; (d) dwell phase.

Four tracer particles were defined in the FE model as shown in Fig. 7. Particle 1 (P1) was set right underneath the pin. Particle 2 (P2) was also located below the pin with a distance of 2 mm to the weld centre. Particle 3 (P3) was located below the shoulder and particle 4 (P4) was located adjacent to the welding tool.
Fig. 8 shows the material flow of these points during the process. The red line is an indicator showing the initial position of the points.

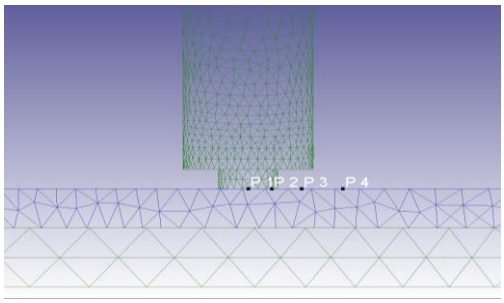

Figure 7. Initial location of the particle tracking.

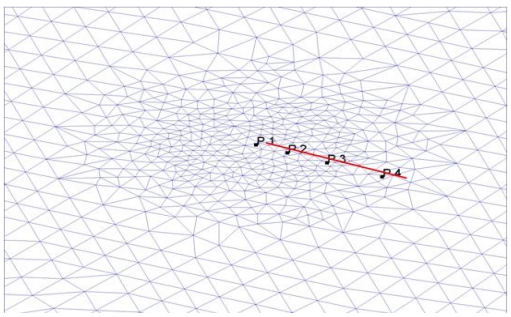

(a)

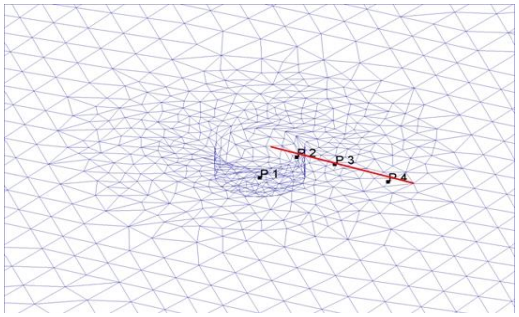

(b)

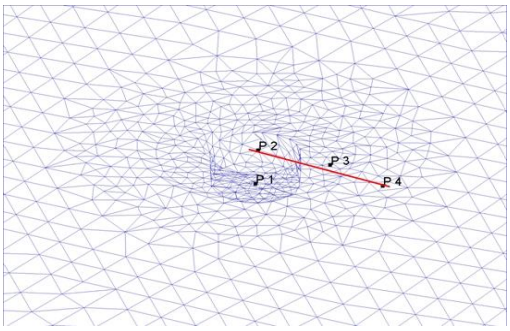

(c)

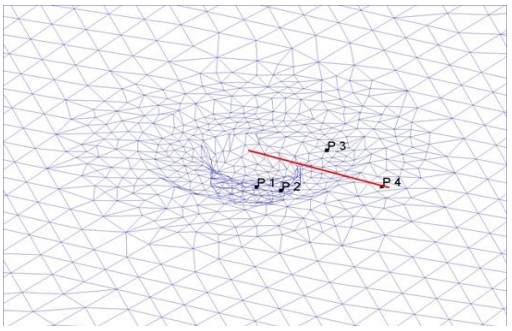

(d)

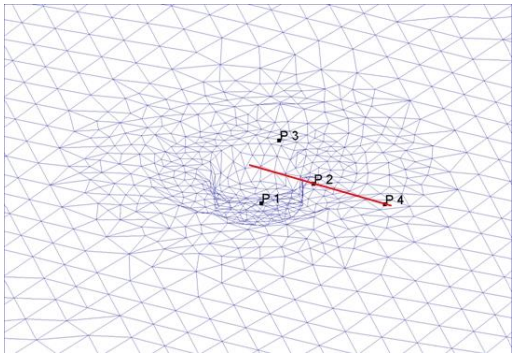

(e)

Figure 8. Material flow at the surface of the work piece: (a) initial location of the tracking particles; (b) compression behaviour of P1 during plunging stage; (c) rotation of the P2 during plunging stage; (d) rotation of the P2 and P3 after shoulder contact and (e) rotation of the P2 and P3 during dwell phase.

It can be concluded from Fig. 8 (b) that the material under the pin mainly experiences the compression process at the beginning of the plunging. After the shoulder contacts with the work piece, P2 starts to rotate with the pin rapidly and P3 has a slight displacement at this time as shown in Fig. 8 (c). By increasing the temperature, the material under the shoulder gets a higher tendency to plastify, and then P3 also rotates with the tool as shown in Fig. 8 (d) and (e).

The displacements of those 4 points are illustrated in Fig. 9 in detail. P1 only moves in Z direction with a displacement of 2.2 mm, which is the predetermined plunge depth. It indicates that the material near the weld centre mainly experiences a serious compression process. For P2, the particle experiences not only the compression process, but also the shear process in X and Y direction. The periodic curve in X and Y direction indicates that the material rotates with the pin. The movement of the material under the shoulder can be seen from Fig. 9 (c). The material moves quite significantly in horizontal plane after the shoulder contacts with the work piece (after 1.67 seconds). Fig. 9 (d) indicates that the material away from the tool has a very small displacement in all directions.

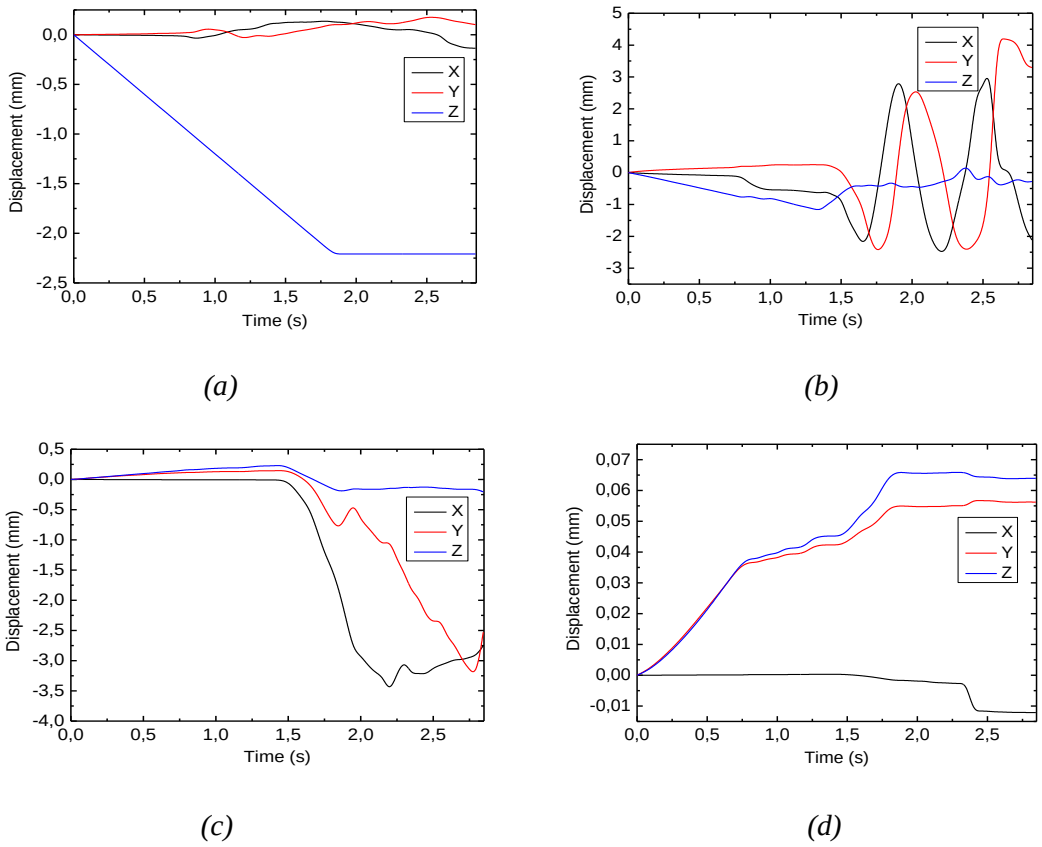

Figure 9. Particle displacement history for tracking points (a) P1; (b) P2; (c) P3 and (d) P4.

4 Conclusions

In this research, a fully coupled thermo-mechanical 3D finite element modeling of FSSW process has been developed. The temperature distribution, effective stain rate as well as the material flow in the joint has been investigated. The main achieved results can be summarized as follows:

(1) The temperature history at the measured points coincided very well between the simulation and experiment results. The peak temperature value in work piece is 526 °C. It is about 0.86 times the homologous melting temperature (in Kelvin) of the base metal. The temperature distribution is symmetric around the tool and the higher temperature appears at the interface between tool and work piece.

(2) The effective strain rate distribution is not uniform. The regions with high effective strain rates are mainly located at the periphery of the pin rather

than the place under the shoulder. At the very beginning of the plunging, the effective strain rate is vey low because there is not enough heat to plastify the material. By plunging the tool, the material obtains a high effective strain rate. Before the shoulder makes contacts with the work piece, the material has already been plasticized and it can obtain a very high effective strain rate.

(3) The material in the weld centre mainly experiences a serious compression process and the other material under the tool experiences both compression and shear process. The material under the shoulder moves quite significantly in horizontal plane after the shoulder has made contacts with the work piece.

References

[1] Mishra, R.S., Ma, Z.Y.: *Friction stir welding and processing*, Materials Science and Engineering R, 50 (2005), 2, 1-78.

[2] Dawes, C. J.: *An introduction to friction stir welding and its development*, Welding and Metal Fabrication, 63 (1995), 1, 13-16.

[3] Klobcar, D., Kosec, L., Pepelnjak, T., et al: *Microstructure and mechanical properties of Friction Stir Welded AlMg4.5Mn alloy*, Engineering Review, 32 (2012), 2, 104-110.

[4] Fujimoto, M., Inuzuka, M., Koga, S.: *Development of friction spot welding*, Welding in the World, 3 (2005), 4, 18-21.

[5] Khosa, S., Weinberger, T., Enzinger, N.: *Finite element analysis of material flow patterns in friction stir spot welding of Al 6082-T6 using different process parameters and tool geometries*, 5th International Conference on Heat Transfer, Fluid Mechanics and Thermodynamics, Sun City, South Africa, 2007.

[6] Gerlich, A., Su, P., North, T.: *Peak temperatures and microstructures in aluminium and magnesium alloy friction stir spot welds*, Science and Technology of Welding and Joining, 10 (2005), 6, 647-652.

[7] Awang, M.: *Simulation of friction stir spot welding (FSSW) process: study of friction phenomena*, Thesis, College of Engineering and Mineral Resources, West Virginia University, 2007.

[8] Assidi, M., Fourment, L., Guerdoux, S., et al: *Friction model for friction stir welding process simulation: calibrations from welding experiments*, International Journal of Machine Tools & Manufacture, 50 (2010), 2, 143-155.

[9] Ji, S., Jin, Y., Yue, Y. et al: *The effect of tool geometry on material flow behavior of friction stir welding of titanium alloy*, Engineering Review, 33 (2013), 2, 107-113.

[10] Buffa, G., Hua, J., Shivpuri, R., et al: *Design of the friction stir welding tool using the continuum based FEM model*, Materials Science and Engineering A, 419 (2006), 1, 381-388.

[11] Asadi, P., Mahdavinejad, R.A., Tutunchilar, S.: *Simulation and experimental investigation of FSP of AZ91 magnesium alloy*, Materials Science and Engineering A, 528 (2011), 21, 6469-6477.